ADVANCED FUNCTIONAL MATERIALS
www.afm-journal.de

Bio-Inspired Multifunctional Metallic Foams Through the Fusion of Different Biological Solutions

Xu Jin, Bairu Shi, Lichen Zheng, Xiaohan Pei, Xiyao Zhang, Ziqi Sun, Yi Du, Jung Ho Kim, Xiaolin Wang, Shixue Dou, Kesong Liu, and Lei Jiang*

Nature is a school for scientists and engineers. Inherent multiscale structures of biological materials exhibit multifunctional integration. In nature, the lotus, the water strider, and the flying bird evolved different and optimized biological solutions to survive. In this contribution, inspired by the optimized solutions from the lotus leaf with superhydrophobic self-cleaning, the water strider leg with durable and robust superhydrophobicity, and the lightweight bird bone with hollow structures, multifunctional metallic foams with multiscale structures are fabricated, demonstrating low adhesive superhydrophobic self-cleaning, striking loading capacity, and superior repellency towards different corrosive solutions. This approach provides an effective avenue to the development of water strider robots and other aquatic smart devices floating on water. Furthermore, the resultant multifunctional metallic foam can be used to construct an oil/water separation apparatus, exhibiting a high separation efficiency and long-term repeatability. The presented approach should provide a promising solution for the design and construction of other multifunctional metallic foams in a large scale for practical applications in the petro-chemical field. Optimized biological solutions continue to inspire and to provide design idea for the construction of multiscale structures with multifunctional integration.

1. Introduction

In 1638, Galileo described bird bones as hollow and lightweight, and modern textbooks state as common knowledge that hollow and lightweight bones in flying birds are a high adaptation to make flight possible.[1–3] For example, the skeleton of bald eagles amounts to only 7% of the body mass, half of what the feathers represent.[4] Many bones in a bird's skeleton are hollow with criss-crossing struts or trusses for structural strength, which is a hierarchically structured composite material. The hollow bones are honeycombed with air spaces, resulting in the increase of buoyancy. This special design provides extra strength and a light weight, which makes it possible to withstand the stresses of taking off, flying, and landing. Metallic foams are a special class of porous materials with a low density and have a combination of mechanical, thermal, electrical and acoustic properties, which have a wide range of applications in the engineering field.[5–8]

The lotus (*Nelumbo nucifera*) is an aquatic plant, living in muddy swamps and ponds. In Asia, the lotus has been a symbol of purity in religions and cultures for more than 2000 years. In order to avoid the leaf decomposition and survive in the aquatic habitats, the lotus leaf shows a self-cleaning effect, that is, the lotus effect, where water droplets can roll freely in all directions and then pick up dirt particles. This can be attributed to the cooperation of surface hydrophobic epicuticular wax and surface multiscale structures with randomly distributed micro-papillae covered by branch-like nanostructures.[9–11] A very high static water contact angle and a very low sliding angle are essential for achieving superhydrophobicity-induced self-cleaning.[12]

Water striders (*Gerris remigis*) are aquatic insects with characteristic length 0.5–1.5 cm and weight 5–10 mg, residing on the surface of ponds, rivers, and the open ocean.[13–15] In order to effortlessly stand, move and jump on the surface of water, water strider legs exhibit durable and robust superhydrophobicity, resulting from their surface multiscale structures in the form of oriented, needle-shaped micro-setae with helical nano-grooves.[14] The leg does not pierce the water surface until a dimple of about 4.3 mm in depth is formed. The maximal

X. Jin, X. Zhang, Prof. K. Liu
Key Laboratory of Bio-Inspired Smart Interfacial Science and Technology of Ministry of Education
School of Chemistry and Environment
Beihang University
Beijing 100191, P. R. China
E-mail: liuks@buaa.edu.cn

X. Jin, B. Shi, L. Zheng, X. Pei
Research Institute of Petroleum Exploration and Development
PetroChina, Beijing 100191, P. R. China

Z. Sun, Y. Du, Prof. J. Kim, Prof. X. Wang, Prof. S. Dou
Institute for Superconducting and Electronic Materials
University of Wollongong
Innovation Campus, Squires Way, North Wollongong
NSW, 2500, Australia

Prof. L. Jiang
Beijing National Laboratory for Molecular Sciences (BNLMS)
Key Laboratory of Organic Solids
Institute of Chemistry
Chinese Academy of Sciences
Beijing 100190, P. R. China

DOI: 10.1002/adfm.201304184

supporting force of a single leg reaches up to 152 dynes, that is, about 15 times the total body weight of a water strider. Therefore, water striders can dance up and down even in turbulent conditions brought by rainstorms or moving water to avoid being drowned and survive on water.

After billions of years of evolution, creatures in nature demonstrate almost perfect structures and functions. Multiscale structures are inherent characteristic for biological materials, exhibiting multifunctional integration.[16–20] Creating multifunctional materials is an eternal goal for human beings. Bio-inspired approaches are proved to be particularly effective. Recently, a great deal of attention has been focused on the development of new multifunctional materials through the fusion of two or more seemingly distinct ideas found in biological materials.[21]

For the lotus, the water strider, and the flying bird, they evolved different and optimized biological solutions to survive. In this contribution, we report the fabrication of bio-inspired multifunctional metallic foams through the fusion of these optimized solutions from the lotus leaf with low adhesive superhydrophobic self-cleaning, the water strider leg with durable and robust superhydrophobicity, and the lightweight bird bone with hollow structures. Three-dimensional (3D) microstructures of the metallic foam with the bird bone-like criss-crossing hollow struts were also revealed using micro X-ray computed tomography (Micro-XCT), a newly-developed in situ imaging technique dedicated to obtaining 3D information non-destructively. Through the construction of multiscale structures followed by the low surface free energy modification, the resultant metallic foams exhibit the low adhesive superhydrophobic self-cleaning, striking loading capacity, and superior repellency towards different corrosive solutions, which offers an effective approach to the development of water strider robots and other aquatic smart devices. An oil/water separation apparatus was also constructed using the multifunctional metallic foam, demonstrating a high separation efficiency and long-term repeatability. Therefore, the presented approach provides an effective solution for the design and construction of other multifunctional metallic foams on a large scale for practical applications in the petro-chemical field. Learning from nature is a promising avenue for scientists and engineers to design and fabricate multifunctional materials.

2. Results and Discussion

Micro-XCT is a kind of newly-developed in situ imaging technique dedicated to obtaining 3D information non-destructively. Typical 3D insight view of the Micro-XCT images of the bird's skeleton and metallic nickel foam are shown in **Figure 1**. The bird's skeleton is porous and hollow from the 3D insight view presented in the Figure 1a. The metallic nickel foam's structure resembles as the bird's skeleton in the 3D insight view in Figure 1b. This special porous metallic foam with a low density and weight should possess considerable buoyancy properties as the bird's bones.

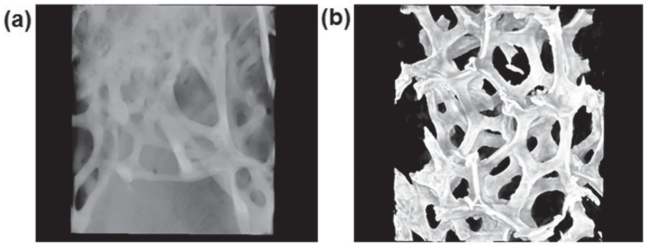

Figure 1. Typical 3D Micro-XCT images of a) the bird's skeleton and b) metallic nickel foam.

Representative environmental scanning electronic microscopy (ESEM) images at different magnifications of metallic nickel foams before and after HNO_3 treatment were shown in **Figure 2**. For the original nickel foam, the low-magnification ESEM image showed its sponge-like porous structure (Figure 2a) and the high-magnification ESEM image demonstrated its surface is smooth and flat (Figure 2b). Nanostructures were not observed on the pristine nickel foam surface. However, for the nickel foam after HNO_3 treatment, binary micro- and nano-scale hierarchical structures were clearly observed. The low-magnification ESEM image shown in Figure 2c exhibited fractal-like rough surface in microscale and the sponge-like porous structure was maintained after the HNO_3 etching. The high magnification ESEM image revealed a rough and disordered network with different sizes and shapes in nanoscale on

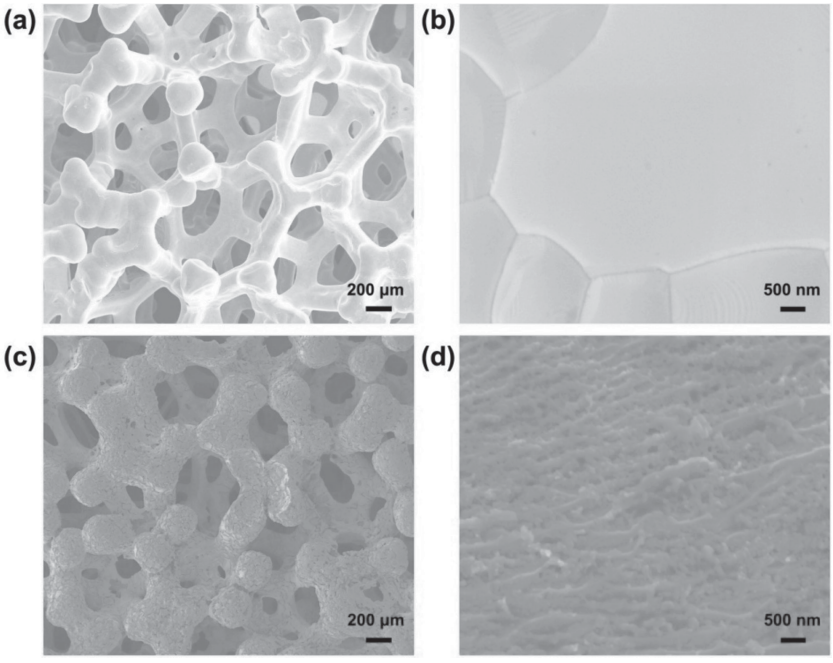

Figure 2. ESEM images of the nickel foam surface before and after the HNO_3 treatment at different magnifications. a–b) ESEM images of the original nickel foam, exhibiting its surface is smooth and flat. c–d) ESEM images of the nickel foam after HNO_3 treatment, showing the resultant surfaces possess micro- and nano-scale hierarchical structures.

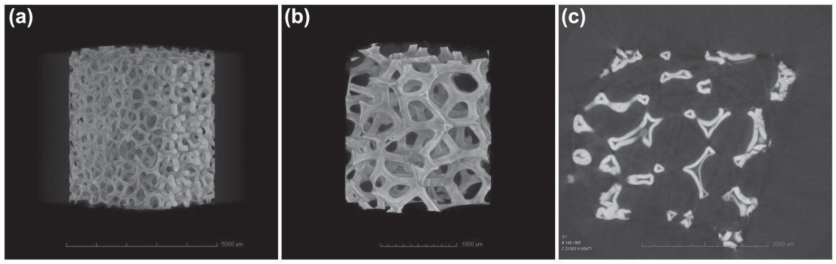

Figure 3. Typical Micro-XCT slices of the metallic nickel foam. a–b) 3D reconstructed Micro-XCT images of metallic faom scanning using 4× and 10× magnification lenses, respectively, showing a 3D open geometry. c) 2D Micro-XCT image of metallic foam, exhibiting the skeleton of the metallic foam is hollow, where the white section is the edges of the foam struts and the black section is air.

the foam surface (Figure 2d). Similar geometrical morphology with random nanostructures can be observed in other superhydrophobic surfaces.[22–24] After the HNO_3 etching, the nickel foam surfaces exhibited multiscale structures, which increased the surface roughness. Binary micro- and nano-scale hierarchical structures are essential for the final formation of superhydrophobicity, as observed in nature on the superhydrophobic surfaces of biomaterials.[10]

For the metallic foam, the ESEM or other 2D morphology is only an oversimplification of its microstructures. In order to meet the increasing need to characterize 3D microstructures of the metallic foam, Micro-XCT was applied to obtain more information about microstructures on the 3D morphology. Representative 3D Micro-XCT slices scanning using 4× and 10× magnification lenses were shown in **Figure 3**a,b, respectively. Micro-XCT images clearly demonstrated the metallic nickel foams possess a 3D open-cellular structure like the sponge (see representative Movies 1,2 in the Supporting Information). The cell distribution is non-periodic. Furthermore, the 2D Micro-XCT slice presented in Figure 3c showed the struts of metallic nickel foams are hollow (see Movie 3 in the Supporting Information). Micro-XCT results demonstrated that sponge-like metallic nickel foams possess the open-cellular morphology and criss-crossing struts with hollow structures, which is similar with the structural features of bird bones in nature (Figure 1).[1–3] These features confer the metallic nickel foam with lightweight and considerable mechanic properties, resulting in the promising applications in the engineering field.[5–8]

For the original nickel foam, the water contact angle is about 80°, exhibiting the intrinsic hydrophilicity (Figure S1a, Supporting Information). After chemical modification with fluoroalkylsilane, the water contact angle of the original nickel foam increased to about 110° (Figure S1b, Supporting Information), demonstrating hydrophobicity. This indicated that the low surface free energy fluoroalkylsilane coating on the original nickel foam increases its water repellent property. However, owing to the insufficient surface roughness, superhydrophobicity cannot be reached. After the HNO_3 treatment, owing to the intrinsic hydrophilicity of the pristine nickel foam, the resultant multiscaled nickel foam with increasing surface roughness without the fluoroalkylsilane modification exhibited superhydrophilicity.[25] The water contact angle is about 0° (Figure S1c, Supporting Information). However, for the nickel foam after the HNO_3 etching followed by the post-modification with low surface free energy fluoroalkylsilane, the case is just contrary. The static water contact angle of the resultant foam is larger than 155°, exhibiting superhydrophobicity (Figure S1d, Supporting Information). The water droplet sitting on the foam surface showed almost a perfect sphere. This can be attributed to the cooperation of surface micro-nanoscale hierarchical roughness and surface fluoroalkylsilane coatings.

In our case, the density of the nickel foam is larger than that of water. Therefore, owing to their higher density and inherent hydrophilicity, the original nickel foams tend to sink beneath the surface of water and finally locate the bottom of the beaker (**Figure 4**a). For the HNO_3-treated nickel foam (4.0 cm × 3.5 cm × 0.3 cm) without the fluoroalkylsilane modification, it will sink the bottom of beaker owing to its superhydrophilicity. According to the Archimedes' principle, the buoyant force (F_B) on an object can be calculated using the following equation:

$$F_B = \rho g V$$

where ρ is the density of the liquid, g is the gravitational acceleration (9.8 m s^{-2}), and V is the volume of the object submerged. The buoyant force on the HNO_3-treated nickel foam without the fluoroalkylsilane modification immersed in water is equal to the weight of the water displaced (1.8 g). It is about 17.64 mN. Therefore, the volume of the superhydrophilic metallic foam submerged under water (V_1) can be expressed as:

$$V_1 = F_B / (\rho g)$$

For water, the density ρ is 1 g mL^{-1}. Therefore, the volume V_1 is about 1.8 mL. However, after modification with fluoroalkylsilane, the resultant superhydrophobic nickel foam (4.0 cm × 3.5 cm × 0.3 cm) can float easily on the water surface (Figure 4b). Fluoroalkylsilane is a typical intrinsically hydrophobic low-surface-energy material. Recent studies demonstrated that, for the superhydrophobic modification, fluoroalkylsilane self-assembled monolayers were formed and covered on the substrate surface.[26–30] A strong bond between the first monolayer of fluoroalkylsilane molecules and the substrate was observed and the thickness of the fluoroalkylsilane layer is less than 2 nm.[31,32] In this case, the weight of the metallic nickel foam is about 6.0 g, that is, the thin fluoroalkylsilane layer adsorbed on the foam can make the metallic foam of 6.0 g in weight float on water. Owing to its heavy weight, the superhydrophobic nickel foam made a clear water dimple on the water surface, exhibiting robust superhydrophobicity. In order to estimate the maximum floating weight of the superhydrophobic metallic nickel foam, the standard weights in different mass were carefully loaded on the foam (Figure 4c–d). Surprisingly, besides its own body weight, the resultant metallic foam can support additional weights of 4.0 g in mass. This indicates the maximal supporting force of the thin fluoroalkylsilane layer in nanoscale coated on the metallic foam can reach 10.0 g. According to the Archimedes' principle, the buoyant force (F_B)

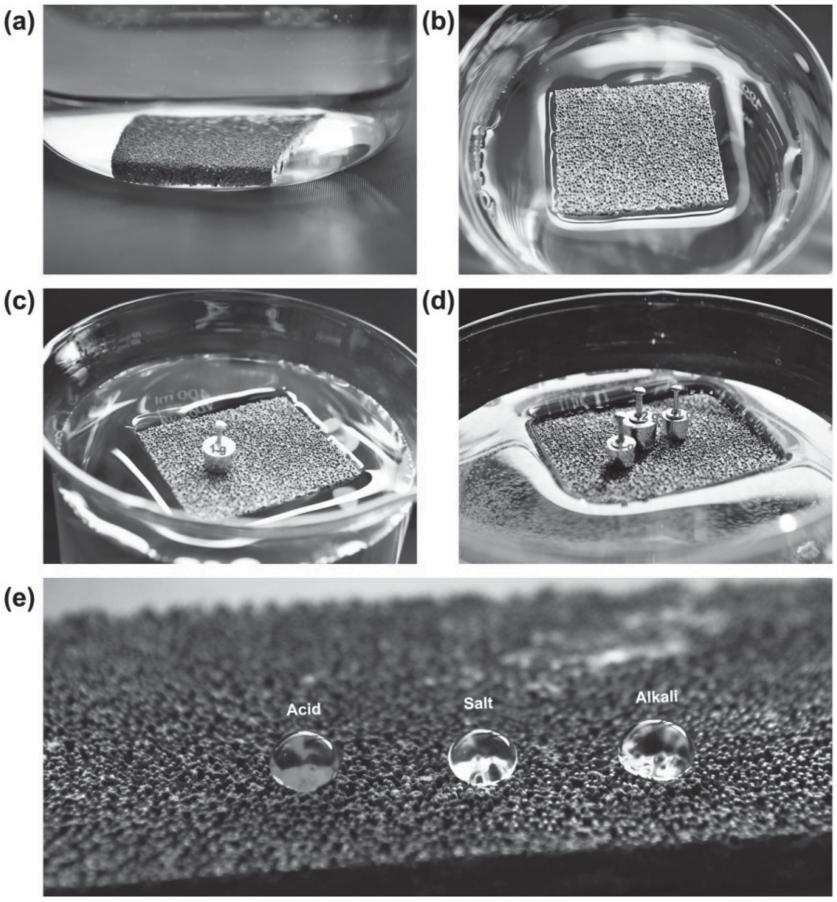

Figure 4. a) Optical image of the original metallic nickel foam sunk the bottom of the water-containing beaker, arising from its heavy weight and inherent hydrophilicity. b) Optical images of the superhydrophobic metallic nickel foam (4.0 cm × 3.5 cm × 0.3 cm, 6.0 g) floating effortlessly on the water surface under different loading weight, b) 0 g; c) 1 g; d) 4 g; exhibiting the striking and robust water-repellent ability similar to the water strider leg found in nature. e) Optical image of aqueous hydrochloric acid (left, pH = 1), NaCl (middle, pH = 7), and NaOH (right, pH = 14) droplets with spherical shapes located on the bio-inspired metallic nickel foam surface, demonstrating the superior repellency towards different corrosive solutions and stable corrosion resistance properties.

on the superhydrophobic metallic foam is about 98 mN, which is more than 5 times the superhydrophilic one (17.64 mN). The ideal depth (h) of the water dimple can be calculated by the deduced Archimedes' principle:

$$V_2 = F_B/(\rho g) = abhh = F_B/(\rho g a b)$$

where a and b are the length (4.0 cm) and the width (3.5 cm) of the superhydrophobic foam, respectively. The ideal depth (h) of the water dimple is about 0.71 cm, which is more than 2 times the thickness (0.3 cm) of the foam. Figure 4d clearly showed a water dimple in high depth surrounding the metallic foam, demonstrating durable and robust superhydrophobicity similar to the water strider leg found in nature. The ability to walk on water is a great dream for human beings. Lightweight metallic foams with striking loading capacity provide a novel solution in the design of water strider robots or other aquatic smart devices working on water.

Metals are important and irreplaceable engineered materials in our society. However, corrosion is headache for metals. Therefore, a great deal of attention has been focused on the development of functional metallic surfaces with stable corrosion resistance properties, which have important industrial applications. In our case, besides the durable and robust superhydrophobicity, the resultant metallic foam also exhibited superior repellency towards corrosive liquids, such as acidic, basic, and some aqueous salt solutions. The static contact angle is almost unchanged over a wide range of pH values from 1 to 14 and even towards corrosive salt solutions, demonstrating the long-term stable stability. Figure 4e shows the typical digital image of acidic (left, pH = 1), salt (middle, pH = 7), and basic (right, pH = 14) droplets on the resultant metallic foam. All these aqueous solution droplets with spherical shapes were located uniformly on the foam even after one month, exhibiting the stable and superior repellency towards different corrosive solutions. The stable corrosion resistance property of the resultant metallic foam can be attributed to the formation of the air layer between the droplet and the foam, which acted as the effective corrosion barrier and inhibited the penetration of the corrosion solution. Metallic foams possessing simultaneous superhydrophobicity and stable anti-corrosion should have important applications in petro-chemical field.

In addition to the considerable loading capacity and stable corrosion resistance properties, the superhydrophobic nickel foam exhibited a low adhesion towards water (Figure S2, Supporting Information). When a water droplet was dropped onto the foam with a tilt angle of less than 10°, the droplet with a ball-like shape rolled easily off the foam surface and dropped into the beaker (see Movie 4 in the Supporting Information). The whole process lasted about 0.4 s. The low adhesive superhydrophobicity of the foam is analogous to that of the lotus leaf in nature, where water drops run freely off their leaves.

In nature, superhydrophobic surfaces can be commonly observed in many plants such as the lotus leaf. Water droplets completely roll off the lotus leaf and carry away dust particles and surface contaminants spontaneously, known as the lotus effect. Owing to the simultaneous superhydrophobicity and low adhesion, the self-cleaning ability of the resultant nickel foam was investigated by sprinkling carbon black as contaminant powders on its surface (Figure S3, Supporting Information). It was found, the water droplet can immediately adsorb contaminant powders as it moved over the foam surface from left to right. Utilizing the water droplet, contaminants were efficiently removed from the foam surface, similar with the lotus effect found in nature. A small water droplet could clean a very long

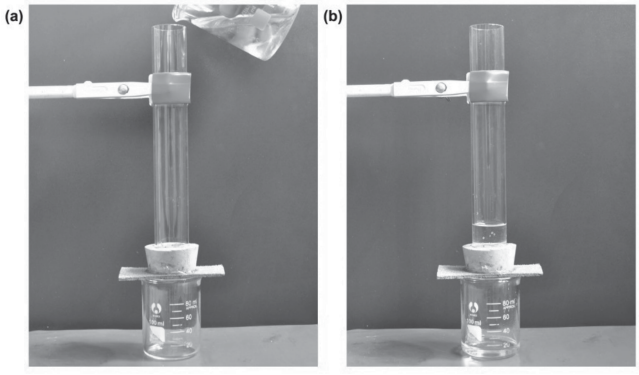

Figure 5. An oil/water separation apparatus constructed by the superhydrophobic metallic foam. a) The mixture of diesel oil and water was put onto the metallic foam. b) Diesel oil quickly permeated through the foam owing to its superoleophilicity and dropped into the beaker below, while water was retained above the foam due to its superhydrophobicity. The oil/water separation efficiency of the metallic foam can reach above 95%.

distance until most of the water droplet was filled by contaminants. During the cleaning process, the ''dirt-containing'' water droplet maintained a spherical shape, where the adsorbed powders could no longer escaped from the water droplet to contaminate the surface again.

Recently, material surfaces with special wettability have attracted a major interest, particularly for the potential industrial applications in the field of oil/water separation.[33–39] Here, utilizing the superhydrophobic and superoleophilic metallic foam, an oil/water separation apparatus was constructed shown in **Figure 5**. The metallic foam was immobilized on the rubber plug, where the vertical glass tube was passed through the rubber plug. When the mixture of diesel oil and water was poured onto the metallic foam, diesel oil quickly permeated through the foam owing to its superoleophilic nature and dropped into the beaker below, while water was retained above the foam due to its superhydrophobic nature. In addition to the diesel oil/water mixture, other oil/water mixtures or organic solvent/water mixtures including crude oil, gasoline and vegetable oil can be effectively separated by using this apparatus. After the separation process, the oil was collected and weighed. The separation efficiency was calculated according to $R = (W_i/W_o) \times 100\%$, where W_o and W_i were the weight of the oil before and after separation process, respectively. The separation efficiency of the metallic foam for a selection of oils is above 95%. This low-cost process can be easily scaled up to separate larger quantities of oil/water mixtures. Furthermore, owing to its self-cleaning effect, the developed oil/water separation apparatus is easily cleaned for reuse. For example, even after 60 separations of the diesel oil/water mixture, the as-prepared metallic foams still retain high separation efficiency (up to 92%, Figure S4, Supporting Information), exhibiting the long-term repeatability, which should have promising practical applications in oil-polluted water treatments.

3. Conclusions

In summary, bio-inspired multifunctional metallic foams were fabricated through the fusion of the different optimized solutions from the lotus leaf with low adhesive superhydrophobic self-cleaning, the water strider leg with durable and robust superhydrophobicity, and the lightweight bird bone with hollow structures. In situ non-destructive Micro-XCT was used to reveal the 3D microstructures of the metallic foam with criss-crossing hollow struts, similar with the structure of the bird bone. The obtained metallic foam exhibited the low adhesive superhydrophobic self-cleaning, striking loading capacity, and superior repellency towards different corrosive solutions, which offers an effective solution to the development of water strider robots and other aquatic smart devices on water. An oil/water separation apparatus was also constructed using the multifunctional metallic foam, demonstrating a high separation efficiency and long-term repeatability. This facile approach for the construction of multifunctional nickel foams possessing superhydrophobicity, self-cleaning, anti-corrosion, and oil/water separation can be extended to fabricate other multifunctional metallic foams on a large scale for the practical applications in the industrial and petro-chemical fields. Learning from nature has proved to be an effective avenue for the design and construction of novel functional materials with multifunction integration.

4. Experimental Section

Multifunctional metallic nickel foams were fabricated through the following approaches. Firstly, the nickel foams were ultrasonically cleaned in absolute alcohol for several minutes to remove oil dirt and then dried at 90 °C for 2 h. The cleaned metallic foams were immersed in 2 M dilute nitric acid at room temperature for 3 h and dried under N_2 stream. Finally, the resultant nickel foams were modified with a 3.0% ethanol solution of fluoroalkylsilane ($CF_3(CF_2)_7CH_2CH_2Si(OCH_3)_3$) for 24 h and heated at 90 °C for 3 h.

Surface morphologies of the samples were characterized by an ESEM (FEI Quanta 250, USA). Water contact angles were measured on a Dataphysics OCA20 (Germany) contact angle system at room temperature. 2-D and 3-D structures of metallic foam were produced using the high resolution Micro-XCT (Xradia Inc. USA). The raw X-ray data was processed by proprietary software (Xradia, Inc.) to generate the 3D reconstructions.

Acknowledgements

The authors appreciate the financial support of National Natural Science Foundation of China (21273016, 21001013), National Basic Research Program of China (2013CB933003, 2010CB934700), Program for New Century Excellent Talents in University, Beijing Natural Science Foundation (2122035), Beijing Higher Education Young Elite Teacher Project, the Fundamental Research Funds for the Central Universities, Australian Research Council (ARC) Discovery Projects (DP1096546, DP140102581), ARC Postdoctoral Research Fellowship, and UOW Vice-chancellor's Research Fellowship.

Received: December 16, 2013
Revised: January 20, 2014
Published online: March 7, 2014

[1] E. R. Dumont, *Proc. R. Soc. B* **2010**, *277*, 2193.
[2] P. Chen, J. McKittrick, M. Meyers, *Prog. Mater. Sci.* **2012**, *57*, 1492.
[3] M. Olszta, X. Cheng, S. Jee, R. Kumar, Y. Kim, M. Kaufman, E. Douglas, L. Gower, *Mater. Sci. Eng. R* **2007**, *58*, 77.

[4] P. Brodkorb, *Wilson Bull.* **1955**, *67*, 142.
[5] J. Banhart, *Prog. Mater. Sci.* **2001**, *46*, 559.
[6] B. H. Smith, S. Szyniszewski, J. F. Hajjar, B. W. Schafer, S. R. Arwade, *J. Constr. Steel Res.* **2012**, *71*, 1.
[7] L. P. Lefebvre, J. Banhart, D. C. Dunand, *Adv. Eng. Mater.* **2008**, *10*, 775.
[8] L. J. Gibson, *Annu. Rev. Mater. Sci.* **2000**, *30*, 191.
[9] W. Barthlott, C. Neinhuis, *Planta* **1997**, *202*, 1.
[10] K. Liu, X. Yao, L. Jiang, *Chem. Soc. Rev.* **2010**, *39*, 3240.
[11] B. Bhushan, Y. C. Jung, *Prog. Mater. Sci.* **2011**, *56*, 1.
[12] K. Liu, L. Jiang, *Annu. Rev. Mater. Res.* **2012**, *42*, 231.
[13] D. L. Hu, B. Chan, J. W. M. Bush, *Nature* **2003**, *424*, 663.
[14] X. F. Gao, L. Jiang, *Nature* **2004**, *432*, 36.
[15] F. Shi, J. Niu, J. Liu, F. Liu, Z. Wang, X. Feng, X. Zhang, *Adv. Mater.* **2007**, *19*, 2257.
[16] P. Podsiadlo, Z. Q. Liu, D. Paterson, P. B. Messersmith, N. A. Kotov, *Adv. Mater.* **2007**, *19*, 949.
[17] K. Liu, L. Jiang, *ACS Nano* **2011**, *5*, 6786.
[18] J. Aizenberg, P. Fratzl, *Adv. Mater.* **2009**, *21*, 387.
[19] K. Koch, B. Bhushan, W. Barthlott, *Prog. Mater. Sci.* **2009**, *54*, 137.
[20] K. Liu, L. Jiang, *Nano Today* **2011**, *6*, 155.
[21] K. Liu, Y. Tian, L. Jiang, *Prog. Mater. Sci.* **2013**, *58*, 503.
[22] H. Erbil, A. Demirel, Y. Avci, O. Mert, *Science* **2003**, *299*, 1377.
[23] K. Liu, Z. Li, W. Wang, L. Jiang, *Appl. Phys. Lett.* **2011**, *99*, 261905.
[24] X. Deng, L. Mammen, H. J. Butt, D. Vollmer, *Science* **2012**, *335*, 67.
[25] R. N. Wenzel, *Ind. Eng. Chem.* **1936**, *28*, 988.
[26] M. Qu, B. Zhang, S. Song, L. Chen, J. Zhang, X. Cao, *Adv. Funct. Mater.* **2007**, *17*, 593.
[27] K. Liu, M. Zhang, J. Zhai, J. Wang, L. Jiang, *Appl. Phys. Lett.* **2008**, *92*, 183103.
[28] T. I. Kim, D. Tahk, H. H. Lee, *Langmuir* **2009**, *25*, 6576.
[29] J. Park, H. Lim, W. Kim, J. S. Ko, *J. Colloid Interface Sci.* **2011**, *360*, 272.
[30] O. Bliznyuk, E. Vereshchagina, E. S. Kooij, B. Poelsema, *Phys. Rev. E* **2009**, *79*, 041601.
[31] A. Hozumi, K. Ushiyama, H. Sugimura, O. Takai, *Langmuir* **1999**, *15*, 7600.
[32] D. Schondelmaier, S. Cramm, R. Klingeler, J. Morenzin, C. Zilkens, W. Eberhardt, *Langmuir* **2002**, *18*, 6242.
[33] G. Kwon, A. K. Kota, Y. Li, A. Sohani, J. M. Mabry, A. Tuteja, *Adv. Mater.* **2012**, *24*, 3666.
[34] Q. Wen, J. C. Di, L. Jiang, J. H. Yu, R. R. Xu, *Chem. Sci.* **2013**, *4*, 591.
[35] X. Zhang, Z. Li, K. Liu, L. Jiang, *Adv. Funct. Mater.* **2013**, *23*, 2881.
[36] W. B. Zhang, Z. Shi, F. Zhang, X. Liu, J. Jin, L. Jiang, *Adv. Mater.* **2013**, *25*, 2071.
[37] Q. Wen, J. C. Di, Y. Zhao, Y. Wang, L. Jiang, J. H. Yu, *Chem. Sci.* **2013**, *4*, 4378.
[38] A. K. Kota, G. Kwon, W. Choi, J. M. Mabry, A. Tuteja, *Nat. Commun.* **2012**, *3*, 1025.
[39] L. B. Zhang, Z. H. Zhang, P. Wang, *Asia Mater.* **2012**, *4*, e8.